Flash sintering of complex shapes

Charles Manière, Geuntak Lee, Eugene A Olevsky

Flash sintering of complex shapes

Charles. Manière[1,2,*,†,‡], Geuntak Lee[1,†], Eugene A. Olevsky[1,*,†]

[1] Powder Technology Laboratory, San Diego State University, San Diego, USA
[2] Normandie Univ, ENSICAEN, UNICAEN, CNRS, CRISMAT, Caen, France
† Powder Technology Laboratory; College of Engineering; San Diego State University; 5500 Campanile Drive; San Diego, CA 92182-1323
‡ Laboratoire de Cristallographie et Sciences des Matériaux (CRISMAT), 6 Blvd du Maréchal Juin 14050 CAEN CEDEX 4, France

Corresponding Authors: charles.maniere@ensicaen.fr, eolevsky@sdsu.edu

Keywords
Flash Sintering; Spark Plasma Sintering; Complex shape; Heat Confinement; Current Concentration

Abstract:

Flash (ultra-rapid) sintering of powder materials is a Multiphysics phenomenon which has a potential for the quasi-instantaneous fabrication of various components. However, the intrinsic instability of flash sintering makes it difficult to apply to complex shapes and large specimens. Here, we circumvent this problem by the use of an interface-controlled approach to impose stable and very fast heating to large powder samples which become fully dense in a matter of seconds. The Multiphysics simulation demonstrated that an electric-thermal-mechanical confinement of the specimen allows a very efficient (and selective) heating and sintering of the powder specimen with a homogeneous microstructure and a substantial reduction of the grain growth. Our results indicate that the ultra-rapid sintering of large and complex shape samples is possible.

Graphical Abstract:

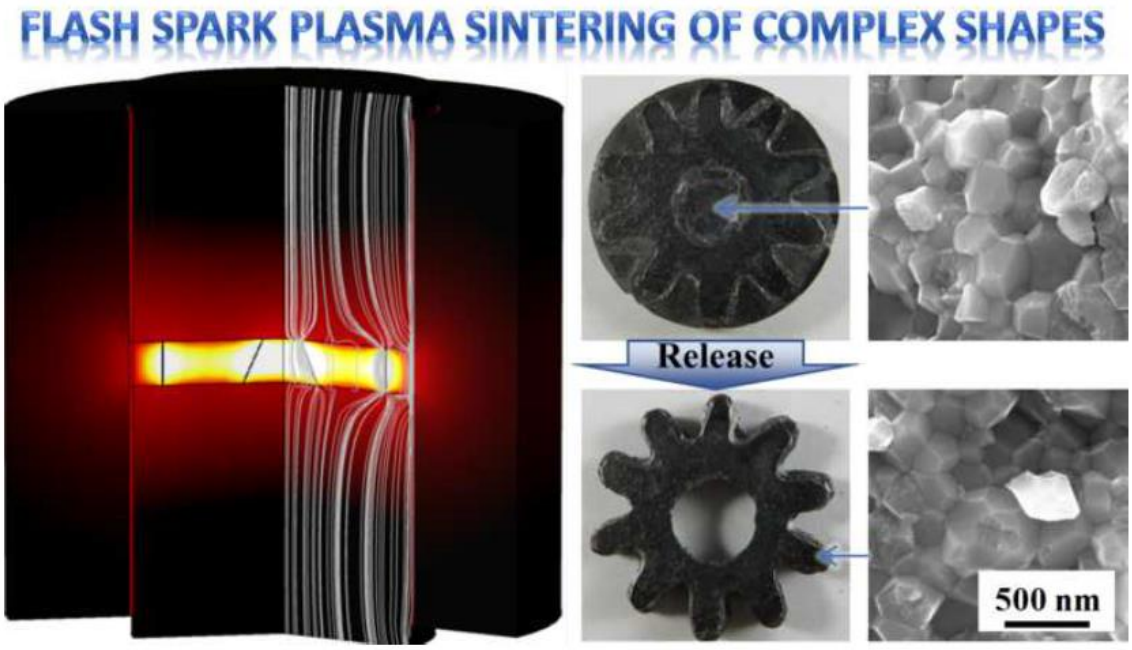

Under high electric current/field, powder materials have demonstrated a particular ability to be consolidated to full density in few seconds[1–3]. The discovery of this phenomenon has been done gradually through the study of the “ultrafast” and “flash” sintering process which involve sintering times below 0.1 s and between 0.1 and 60 s, respectively[4,5]. Ultrafast high voltage compaction/sintering uses an electric discharge pulse from a capacitor bank to sinter/consolidate conductive powders[6]. In 2010, the work of Cologna et al.[1] introduced “flash sintering” as a field assisted sintering process which involves electric fields between 7.5 and 1000 V/cm with a power dissipation of 10 to 1000 mW/mm^3, and “wherein the onset of sintering is accompanied by a non-linear increase in the conductivity of the material”[1]. This runaway phenomenon accompanied by densification in less than a minute is a typical behavior of materials with the negative temperature coefficient (NTC), such as zirconia.

Since the advent of flash sintering, this technique has been successfully implemented in advance processes such as Spark Plasma Sintering or microwave sintering for a broad spectrum of materials[4,7–9].

For microwave sintering, the direct interaction of the microwaves and the matter enables a very fast heating and sintering of ceramic[7] and metal[10,11] powders. The main advantage of the microwave flash sintering is in its contactless and volumetric heating nature. However, this process suffers from a high inherent heating instability. The NTC behavior of some materials implicates a greater heat dissipation in the hot areas, which tends to amplify the heating instabilities creating hot spot phenomena[12,13]. In the field assisted sintering approaches, the incidents of the localized electric current concentration and localized heating are reported[5,13] which significantly limit the treatable size of the flash sintered specimens, which are generally few millimeters thick dog bone shape samples.

Because of these thermal instabilities, the idea of utilizing the flash sintering process for the fabrication of large and complex shape components seems very difficult to implement. An exception is the lattice structures or 2D shapes[14] ensuring homogeneous electric current density that has been flash treated via reactive sintering[15]. However, the new adaptation of flash sintering to the spark plasma sintering (SPS), which integrates a die pressing and a pulsed current Joule heating, opens new interesting and very promising possibilities. The flash spark plasma sintering (FSPS) is an approach using a sinter-forging configuration able to preheat the specimen to activate flash sintering that can be applied to various NTC materials such as SiC specimen as large as 60 mm in diameter[9,16]. In the work of Zapata-Solvas et al[17], an electrically insulated die is used to have better control of the sample shape while concentrating the current in the powder area, which provides close to flash sintering conditions. We previously[8] employed a similar configuration (reported in Fig. 1a) to show that an ultra-rapid sintering can be enacted for any kind of powder regardless of its electrical conductivity (from electrically insulative highly pure alumina to metals like nickel) via an imposed electric current control. We obtained 10 mm diameter net shape pellets with a very homogeneous microstructure. We showed also by the finite element simulation that this homogeneity is due to the combination of the thermal confinement by the lateral thermal contact resistance and the hybrid heating where the lateral graphite foil dissipates an external heating which plays a role similar to susceptor (by analogy with microwave sintering). The powder can be considered to be electro-thermally and mechanically confined.

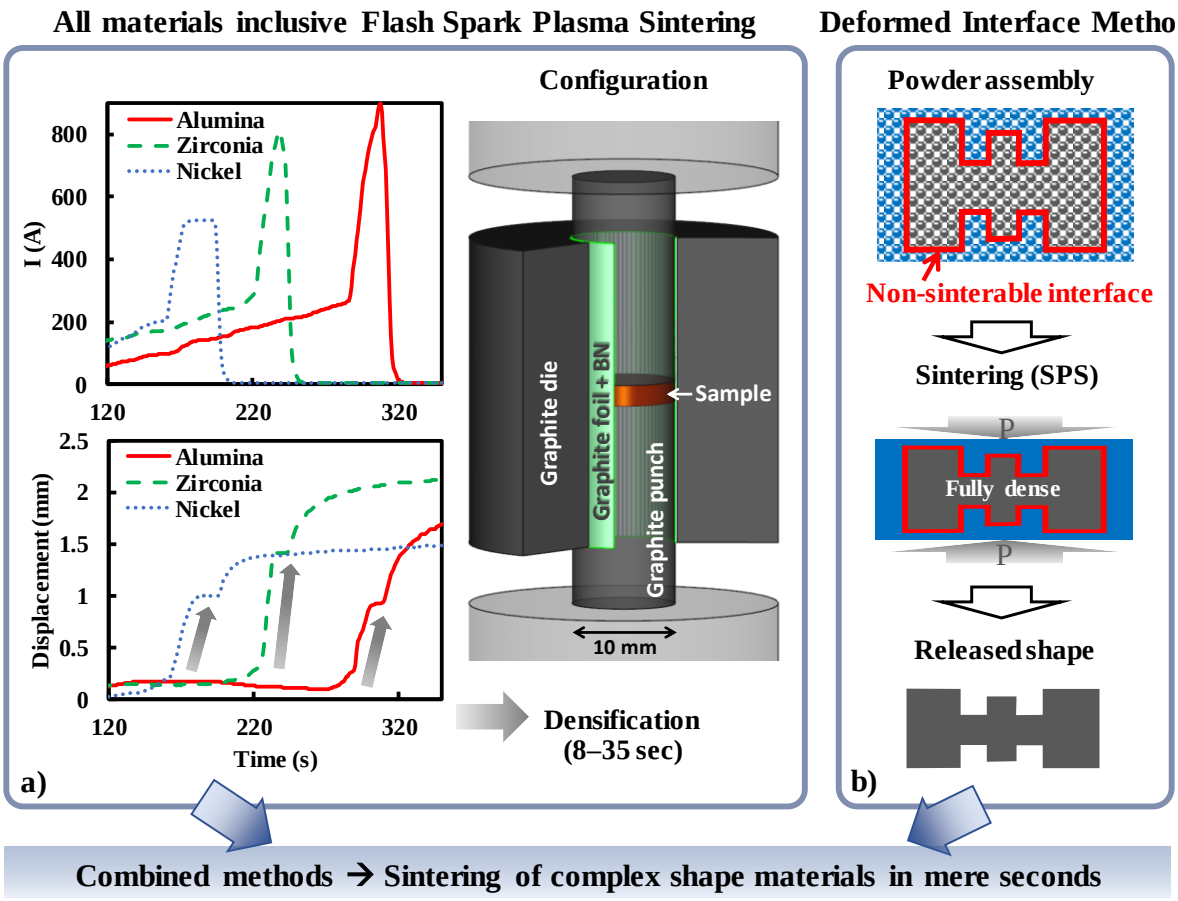

Fig. 1 Concept of complex shape flash sintering. The ultra-rapid complex shape sintering method integrates two coupled approaches: a) the flash spark plasma sintering conditions and configuration[8] *b) the complex shape deformed interface approach*[18].

The typical hybrid heating within this setup makes it suited for larger-scale applications of flash sintering. In addition, the mechanical confinement (provided by the die) helps to impose a uniform displacement field in the specimen. We recently showed that this FSPS concept can be applied to larger specimens of 30 mm [19]. This opens a very interesting opportunity for the fabrication of complex shapes through the "deformed interface approach"[18] enabling specimens with size of at least 15-30mm to be handled. In this approach (represented in Fig. 1b), an assembly of powders separated by a deformable interface is employed. This method (described in the "Method" section) is based on the mutual densification of the complex shape fabricated parts and sacrificial parts, which results in the possibility to fully sinter complex shape objects. When used under spark

plasma sintering, this approach has already shown the ability to generate fully dense shapes, as complex as turbine blades, regular and twisted gear shapes, etc. (see Fig. 2).

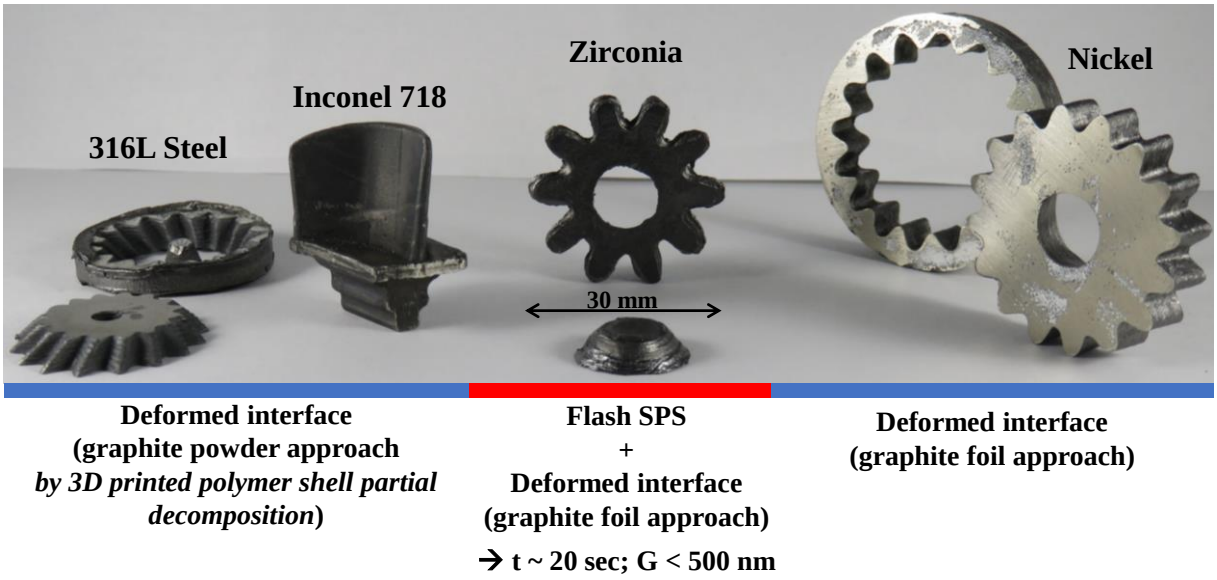

Fig. 2 Complex shape parts obtained by the deformed interface approach and in combination with the flash spark plasma sintering approach.

Thus, the combination of the "Flash Spark Plasma Sintering" conditions (which we showed to be "all materials inclusive"[8]) and the "Deformable Interface Approach" (which has been shown to be "all shape inclusive"[18]) enables the flash sintering of complex shapes. In other words, the fabrication of complex shapes from powder materials in a few seconds becomes possible. This interface-aided flash sintering approach may be coupled with the recently developed volumetric[20], continuous[21], multi-materials additive manufacturing methods with printing time of seconds or minutes to generate the graphite interfaces after the polymeric *in situ* decomposition[22].

In the following description, we will discuss first the probable physical basis of this ultra-rapid sintering technique. Then we will consider in detail the results of our first fabrication of the flash sintered complex shape.

Based on the continuum theory of sintering[23], the classical low heating rate (10 K/min) sintering models fail to explain the ultra-rapid densification of the same materials when

high heating rates are used up to the temperature close to the melting point[11]. This suggests the presence of additional phenomena responsible for such an acceleration of the sintering kinetics. The physical origin of these additional factors is still intensely debated. In particular, localized heating at preferential sites, such as grain boundaries and particle surfaces, was considered by Cologna et al[1]. Despite the high diffusivity of the heat in small size particles[24] contradicts this hypothesis, melted or softened grain boundaries have been observed for SPS[25] and microwave[7] sintering. Another main mechanism is the influence of the electric current and temperature on the defects' nucleation (vacancy, dislocation, Frenkel pairs, etc.) causing the potential enhancement of the sintering mass transport. Defects can affect the dislocation motion intensifying local Joule heating and therefore create more defects. Using the electro-plasticity approach, we analyzed this phenomenon for conductive powders during SPS[26,27]. In the following equation, the deformability term A is the sum of the thermal $A(T)$ and non-thermal $A(J)$ terms where the cumulative thermal energy at the defects is taken into account[26]:

$$\dot{\theta} = -[A(T) + A(J)]\left(\frac{3\theta}{2}\right)^{\frac{m+1}{2m}}(1-\theta)^{\frac{m-1}{2m}}\left(\frac{\sigma_z}{G}\right)^{\frac{1}{m}} \quad (1)$$

$$A(J) = \beta^{\omega}\left[\int_{t_0}^{t_f}\frac{J_L^2\lambda}{G}dt\right]^{\omega} \quad (2)$$

where θ is the porosity, m is the strain rate sensibility, σ_z is the applied stress, G is the shear modulus, J_L is the local electric current density, λ is the electrical resistivity, and ω is the electric current sensitivity exponent.

Finally, the case of the ultra-rapid densification of a highly pure alumina (Fig. 1a) highlights a different aspect of the flash sintering that involves the enhancing effect of the high heating rates (without the contribution of the electric current). It has been shown that fast firing, such as using Ni and Al exothermic reaction, can lead to an ultra-rapid densification (without electric current) of zirconia[28], similar to flash sintering. This can

be due to the preservation of the early stage high reactivity due to the retention of non-equilibrium grain boundaries[29,30] or pore coarsening[31].

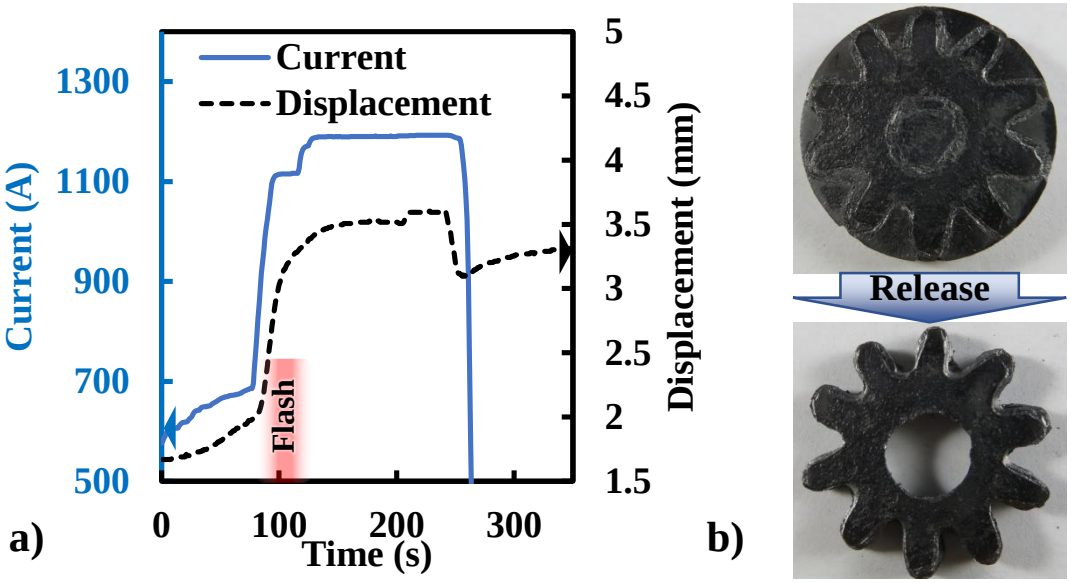

Fig. 3 Flash sintering of 30 mm zirconia gear. a) Current and displacement curves recorded during the flash spark plasma sintering experiment b) the upper part shows the sintered pellet where the gear shape appears along with the sacrificial parts and graphite foils interface, the lower part shows the released gear shape after ejection of the sacrificial parts.

The first prototype of the flash sintered complex shape is a 30 mm diameter zirconia gear. This case addresses the problem of the thermal stability during flash sintering of large specimens and its capacity to generate complex shapes. The powder assembly process uses a graphite foil skeleton and is described in detail in the Method section. The flash conditions are based on a strategy similar to the one employed in the 10 mm size specimen (Fig. 1a): a rapid increase of the electrical current is applied (see Fig. 3a). In this case, the electric current is held longer time after reaching the maximum density to ensure the stable heating and uniform microstructure. The densification is very fast and takes roughly 20 s during the electric current increase after taking additional 20 s to stabilize. The flash sintered zirconia specimen is reported in Fig. 3b; the flash sintered pellet with the graphite foil interfaces is shown in the upper image. After ejecting the sacrificial parts, the gear shape is finally obtained. The simulation of this experiment (Fig. 4) shows a very selective

heating in the specimen where the electric current lines passing through the graphite foil extend to the powder that becomes conductive at high temperatures[2]. The grain sizes obtained in the center and at the edge of the sample are largely under 500 nm and very homogeneous. The temperature differences in the sample are about 100 K but it appears that the short sintering time prevents microstructure non-uniformity. Another interesting aspect is the transition from white to black zirconia. Zirconia is an ionic conductor and under the vacuum reducive conditions of SPS, it transforms to black zirconia [32] and becomes an electronic conductor that can ensure a volumetric heating of the powder. The contact with graphite elements significantly increases these reduction phenomena. The sensitivity to this transformation can be reduced by AC current [33,34]. However, the improvement of zirconia electric and thermal conductivity, when becoming black zirconia, has a stabilizing effect on the thermal distribution, and, at the same time, the mechanical properties of black zirconia are still high [35,36]. To determine the mechanical resistance of black zirconia, SPS sintered white and black zirconia specimens have been compared *via* 100K/min (white) and 1000K/min (black) experiments (on 15 mm pellets [19]). We obtain similar values of Vickers hardness and toughness; $HV_{2.0}$ 12.25 ± 0.23 GPa, K_{Ic} 5.70 ± 0.14 MPa $m^{1/2}$ for white zirconia and $HV_{2.0}$ 13.45 ± 0.13 GPa, K_{Ic} 5.62 ± 0.13 MPa $m^{1/2}$ for black zirconia. These values are close to those obtained for the same powder by conventional sintering (1400°C); $HV_{2.0}$ 12.54 ± 0.23 GPa, K_{Ic} 4.88 ± 0.28 MPa $m^{1/2}$ [37].

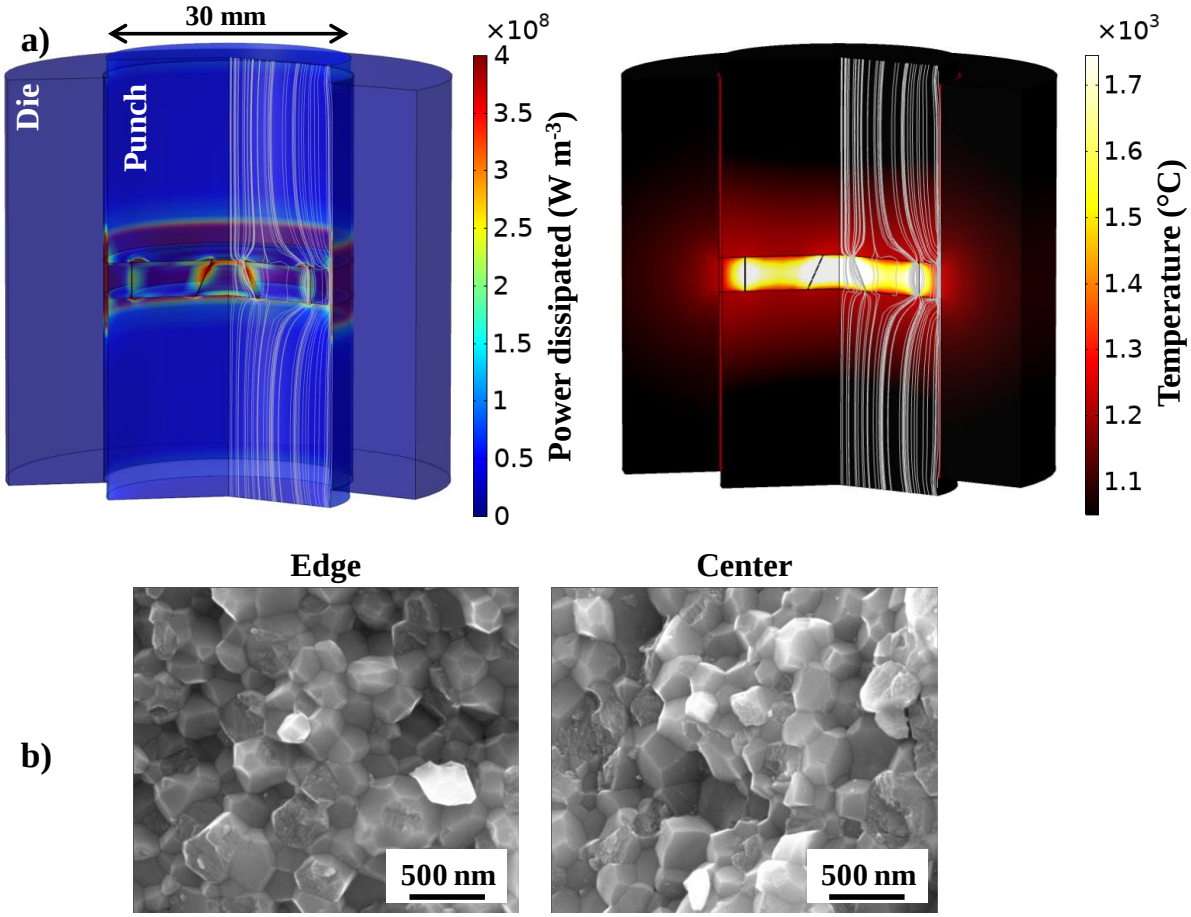

Fig. 4 Physical field uniformity and correlation with obtained microstructures. The upper part (a) shows the temperature distribution and electric current lines during the electric current peak, the lower part (b) represents the SEM fracture images in the center and at the edge of the sintered sample which demonstrate a homogeneous microstructure with grain size clearly lower than 500 nm.

To conclude, the flash sintering conditions, traditionally utilized in small size specimens, are possible to implement, based on the interface aided flash sintering, in larger scale specimens resulting in homogeneous microstructures with very limited grain growth. The heating appears to be very selectively concentrated in the specimen which makes the process very energy efficient. The electrically insulated die enables a very homogeneous and predictable displacement field in the powder which allows applying the deformable interface method to fabricate any kind of complex shapes.

Methods

The flash spark plasma sintering approach: Our flash SPS approach uses a die & punches configuration (reported in figure 1a), where graphite foil is introduced in the vicinity of the punch/die and sample/die interfaces. In order to concentrate the electric current in the area of the powder, the inner die hole is electrically insulated by the boron nitride spray coated directly on the external graphite foil surface. In this way, the electric current can flow in the powder, or to the surrounding graphite foil, if the powder has too low conductivity. For the flash SPS of zirconia, this configuration allows preheating through the graphite foil to activate the onset of the flash sintering helping the transition from the low conductivity of the powder at room temperature to the higher conductivity at high temperatures. For electrically insulative powders, (such as highly pure alumina), the graphite foil becomes the main heating element in direct contact with the powder which also allows an ultra-rapid densification. The graphite foil helps stabilize the heating during the flash regime, by providing a highly localized additional and external heating. Larger specimens can then be flash sintered thanks to this hybrid heating.

In the traditional flash sintering approach, the negative temperature coefficient (NTC) behavior of materials, such as zirconia or silicon carbide, causes a thermal runaway heating profile accompanied by an ultra-rapid densification[13,38]. In order to impose an ultra-rapid densification regardless of the powder conductivity, we impose directly a spike of the electric current controlling its intensity and holding time to generate an imposed ultra-rapid heating and sintering profile. For 10 mm specimen (figure 1a) we imposed a simple peak of the electric current up to the full density without holding time. For 30 mm specimen with the inner complex shape, we hold the electric current for a longer time to ensure a spatially stable heating.

The spark plasma sintering experiments were performed (using the SPS device SPSS DR.SINTER Fuji Electronics model 5015) under constant pressure of 90 MPa for the 10 mm specimens and 50 MPa for the 30 mm gear experiment. The following powders have been used: a highly pure alumina as the electrically insulative powder (Cerac, Al_2O_3 99.99 % pure, 37 nm), nickel as the conductive powder (Cerac, Ni 99.9% pure, 5 μm), and a partially yttria stabilized zirconia powder 3Y-ZrO_2 (Tosoh- zirconia TZ- 3YS, 100 nm) has been used as the intermediate conductivity powder with NTC behavior.

Deformed interface approach for complex shapes: This approach includes three main steps reported in figure 1b: 1) the powder assembly of at least two powder areas separated by a non-sinterable, deformable interface is generated, 2) the powder assembly is sintered by a die compaction method such as “hot pressing” or “spark plasma sintering”. During this step, the separation interface follows the mutual densification of the powders. 3) The last step is the ejection of the sacrificial parts, which is possible thanks to the internal separation interface[39]. This interface can be made of a powder (graphite, oxides, nitrides, carbides) or a semi-rigid foil skeleton and should be able to accompany the mutual displacement of the fabricated complex shape part and the sacrificial area during sintering without significantly disturbing the displacement field. Using 3D printing of a polymer shell, it is possible to generate directly a graphite powder separation interface between the powders after partial decomposition of the polymer during the heating in SPS device (for oxygen-free atmosphere)[22]. By this approach very complex shell architecture geometries (figure 2) can be 3D printed to ease the ejection of the shapes and allow multiple parts production. Powders in both areas should be ideally the same to ensure the homogeneous specimen’s displacement field. However, for cost efficiency, the powder of the sacrificial area can be different, although the densification behavior of both powders should be as close as possible. The shape surface aspect depends on the nature of the printed interface or

the graphite tool in contact. An additional powder bed can be placed at the punch/sample interface to ease the sample ejection. This may create some surface roughness (nickel gears figure 2) that can be improved by polishing or sandblasting.

This approach addresses the problem of thickness variation in the die compaction process, where the high thickness areas are generally very difficult to fully densify as they need more shrinkage than the lower thickness zones[40]. Solving this problem requires complicated multiple punches approaches[41,42] eventually using sacrificial materials[43]. The advantage of this approach is to use a regular compaction tooling which, with the addition of complex separation interfaces, can be designed to generate complex shape parts and/or multiple part specimens simultaneously densified. The non-restrictive nature of the internal interface design makes this approach “all shape inclusive”.

Combined flash of deformed interfaces approaches: The combined approach utilized in this work renders the flash spark plasma sintering conditions in a 30 mm diameter cylindrical working space with graphite foil interfaces introduced for the creation of a complex shape zirconia gear. To increase the thermal confinement of the heat generated in the powder, two graphite foils are added in the lateral punch/die and sample/die interfaces; and, to reduce the cooling flux through the sample/punches interfaces, three graphite foils are introduced. The gear shape has been imposed via the graphite foils with the help of a 3D printed (GEEETech prusa i3) polymer (ABS) gear mold. The zirconia powder is then filled around the graphite foil skeleton to apply the “deformed interface approach”. Each step of the preparation from the 3D printed ABS gear with desired shape to finial flash sintered zirconia gear is reported in supplementary material. As shown by the simulation figure 4, the heat is guided by the inner graphite separation interface and is propagated to the rest of the powdered specimen due to the high electrical conductivity of zirconia at high temperature. At high temperature and for oxygen-deficient conditions, the flash

sintered zirconia specimen may become highly electronically conductive due to an electrochemical reduction[34].

Electro-thermal-mechanical (ETM) finite element simulation: The ETM model predicts both the Joule heating of the SPS Pressing column and the densification of the powder. The governing equations and boundary conditions are fully described in ref[40,44]. The electric and thermal contact resistances (ECR and TCR) in all the interfaces have a significant impact on the thermal field and the heat confinement of the powder[45,46]; the values of the ECR and TCR are based on ref[47]. In the interfaces with several graphite foils, the ECR and TCR have been calculated accounting for the equivalent electric and thermal resistance of each graphite foil.

References

[1] M. Cologna, B. Rashkova, R. Raj, Flash Sintering of Nanograin Zirconia in <5 s at 850°C, J. Am. Ceram. Soc. 93 (2010) 3556–3559. doi:10.1111/j.1551-2916.2010.04089.x.

[2] M. Biesuz, V.M. Sglavo, Flash sintering of ceramics, J. Eur. Ceram. Soc. 39 (2019) 115–143. doi:10.1016/j.jeurceramsoc.2018.08.048.

[3] C.E.J. Dancer, Flash sintering of ceramic materials, Mater. Res. Express. 3 (2016) 102001. doi:10.1088/2053-1591/3/10/102001.

[4] M. Yu, S. Grasso, R. Mckinnon, T. Saunders, M.J. Reece, Review of flash sintering: materials, mechanisms and modelling, Adv. Appl. Ceram. 116 (2017) 24–60. doi:10.1080/17436753.2016.1251051.

[5] E.A. Olevsky, D. V. Dudina, Field-Assisted Sintering, Springer N, Springer International Publishing, Cham, 2018. doi:10.1007/978-3-319-76032-2.

[6] M.S. Yurlova, V.D. Demenyuk, L.Y. Lebedeva, D. V. Dudina, E.G. Grigoryev, E.A. Olevsky, Electric pulse consolidation: an alternative to spark plasma sintering, J. Mater. Sci. 49 (2014) 952–985. doi:10.1007/s10853-013-7805-8.

[7] Y. Bykov, S. Egorov, A. Eremeev, V. Kholoptsev, I. Plotnikov, K. Rybakov, A. Sorokin, On the Mechanism of Microwave Flash Sintering of Ceramics, Materials (Basel). 9 (2016) 684. doi:10.3390/ma9080684.

[8] C. Manière, G. Lee, E.A. Olevsky, All-Materials-Inclusive Flash Spark Plasma Sintering, Sci. Rep. 7 (2017) 15071. doi:10.1038/s41598-017-15365-x.

[9] E.A. Olevsky, S.M. Rolfing, A.L. Maximenko, Flash (Ultra-Rapid) Spark-Plasma Sintering of Silicon Carbide, Sci. Rep. 6 (2016) 33408. doi:10.1038/srep33408.

[10] J. Perelaer, M. Klokkenburg, C.E. Hendriks, U.S. Schubert, Microwave Flash Sintering of Inkjet-Printed Silver Tracks on Polymer Substrates, Adv. Mater. 21 (2009) 4830–4834. doi:10.1002/adma.200901081.

[11] C. Manière, G. Lee, T. Zahrah, E.A. Olevsky, Microwave flash sintering of metal powders: From experimental evidence to multiphysics simulation, Acta Mater. 147 (2018) 24–34. doi:10.1016/j.actamat.2018.01.017.

[12] C. Manière, T. Zahrah, E.A. Olevsky, Inherent heating instability of direct microwave sintering process: Sample analysis for porous 3Y-ZrO2, Scr. Mater. 128 (2017) 49–52. doi:10.1016/j.scriptamat.2016.10.008.

[13] R.I. Todd, E. Zapata-Solvas, R.S. Bonilla, T. Sneddon, P.R. Wilshaw, Electrical characteristics of flash sintering: thermal runaway of Joule heating, J. Eur. Ceram. Soc. 35 (2015) 1865–1877. doi:10.1016/j.jeurceramsoc.2014.12.022.

[14] B. Yang, J. Cho, X.L. Phuah, H. Wang, X. Zhang, Flash sintering of additively manufactured 3YSZ gears, J. Am. Ceram. Soc. 104 (2021) 3828–3832. doi:10.1111/jace.17835.

[15] C. Wang, W. Ping, Q. Bai, H. Cui, R. Hensleigh, R. Wang, A.H. Brozena, Z. Xu, J. Dai, Y. Pei, C. Zheng, G. Pastel, J. Gao, X. Wang, H. Wang, J.-C. Zhao, B. Yang, X. (Rayne) Zheng, J. Luo, Y. Mo, B. Dunn, L. Hu, A general method to synthesize and sinter bulk ceramics in seconds, Science (80-.). 368 (2020) 521–526. doi:10.1126/science.aaz7681.

[16] S. Grasso, T. Saunders, H. Porwal, B. Milsom, A. Tudball, M. Reece, Flash Spark Plasma Sintering (FSPS) of α and β SiC, J. Am. Ceram. Soc. 99 (2016) 1534–1543. doi:10.1111/jace.14158.

[17] E. Zapata-Solvas, D. Gómez-García, A. Domínguez-Rodríguez, R.I. Todd, Ultra-fast and energy-efficient sintering of ceramics by electric current concentration, Sci. Rep. 5 (2015) 8513. doi:10.1038/srep08513.

[18] C. Manière, E. Nigito, L. Durand, A. Weibel, Y. Beynet, C. Estournès, Spark plasma sintering and complex shapes: The deformed interfaces approach, Powder Technol. 320 (2017) 340–345. doi:10.1016/j.powtec.2017.07.048.

[19] C. Manière, C. Harnois, G. Riquet, J. Lecourt, C. Bilot, S. Marinel, Flash spark plasma sintering of zirconia nanoparticles: Electro-thermal-mechanical-microstructural simulation and scalability solutions, J. Eur. Ceram. Soc. (2021). doi:10.1016/j.jeurceramsoc.2021.09.021.

[20] B.E. Kelly, I. Bhattacharya, H. Heidari, M. Shusteff, C.M. Spadaccini, H.K. Taylor, Volumetric additive manufacturing via tomographic reconstruction, Science (80-.). 363 (2019) 1075–1079. doi:10.1126/science.aau7114.

[21] M. Zastrow, 3D printing gets bigger, faster and stronger, Nature. 578 (2020) 20–23. doi:10.1038/d41586-020-00271-6.

[22] C. Manière, E.A. Olevsky, In situ partially degradable separation interface for fabrication of complex near net shape objects by pressure assited sintering, Patent US 2021/0016499 A1, US2021/0016499A1 WO2019/191299A1, 2018.

[23] E.A. Olevsky, Theory of sintering: from discrete to continuum, Mater. Sci. Eng. R Reports. 23 (1998) 41–100. doi:10.1016/S0927-796X(98)00009-6.

[24] T.B. Holland, U. Anselmi-Tamburini, D. V. Quach, T.B. Tran, A.K. Mukherjee, Effects of local Joule heating during the field assisted sintering of ionic ceramics, J.

Eur. Ceram. Soc. 32 (2012) 3667–3674. doi:10.1016/j.jeurceramsoc.2012.02.033.

[25] R. Chaim, C. Estournès, On thermal runaway and local endothermic/exothermic reactions during flash sintering of ceramic nanoparticles, J. Mater. Sci. 53 (2018) 6378–6389. doi:10.1007/s10853-018-2040-y.

[26] G. Lee, E.A. Olevsky, C. Manière, A. Maximenko, O. Izhvanov, C. Back, J. McKittrick, Effect of electric current on densification behavior of conductive ceramic powders consolidated by spark plasma sintering, Acta Mater. 144 (2018) 524–533. doi:10.1016/j.actamat.2017.11.010.

[27] G. Lee, C. Manière, J. McKittrick, E.A. Olevsky, Electric current effects in spark plasma sintering: From the evidence of physical phenomenon to constitutive equation formulation, Scr. Mater. 170 (2019) 90–94. doi:10.1016/j.scriptamat.2019.05.040.

[28] W. Ji, B. Parker, S. Falco, J.Y. Zhang, Z.Y. Fu, R.I. Todd, Ultra-fast firing: Effect of heating rate on sintering of 3YSZ, with and without an electric field, J. Eur. Ceram. Soc. 37 (2017) 2547–2551. doi:10.1016/j.jeurceramsoc.2017.01.033.

[29] P.R. Cantwell, S. Ma, S.A. Bojarski, G.S. Rohrer, M.P. Harmer, Expanding time–temperature-transformation (TTT) diagrams to interfaces: A new approach for grain boundary engineering, Acta Mater. 106 (2016) 78–86. doi:10.1016/j.actamat.2016.01.010.

[30] J. Zhang, F. Meng, R.I. Todd, Z. Fu, The nature of grain boundaries in alumina fabricated by fast sintering, Scr. Mater. 62 (2010) 658–661. doi:10.1016/j.scriptamat.2010.01.019.

[31] E.A. Olevsky, S. Kandukuri, L. Froyen, Consolidation enhancement in spark-plasma sintering: Impact of high heating rates, J. Appl. Phys. 102 (2007) 114913. doi:10.1063/1.2822189.

[32] T.P. Mishra, R.R.I. Neto, G. Speranza, A. Quaranta, V.M. Sglavo, R. Raj, O. Guillon, M. Bram, M. Biesuz, Electronic conductivity in gadolinium doped ceria under direct current as a trigger for flash sintering, Scr. Mater. 179 (2020) 55–60. doi:10.1016/j.scriptamat.2020.01.007.

[33] M.C. Steil, D. Marinha, Y. Aman, J.R.C. Gomes, M. Kleitz, From conventional ac flash-sintering of YSZ to hyper-flash and double flash, J. Eur. Ceram. Soc. 33 (2013) 2093–2101. doi:10.1016/j.jeurceramsoc.2013.03.019.

[34] M. Biesuz, L. Pinter, T. Saunders, M. Reece, J. Binner, V. Sglavo, S. Grasso, Investigation of Electrochemical, Optical and Thermal Effects during Flash Sintering of 8YSZ, Materials (Basel). 11 (2018) 1214. doi:10.3390/ma11071214.

[35] J. Xu, Z. Liu, Z. Xie, S. He, X. Xi, DC electric field-assisted hot pressing of zirconia: methodology, phenomenology, and sintering mechanism, J. Am. Ceram. Soc. (2021) jace.17963. doi:10.1111/jace.17963.

[36] G.M. Jones, M. Biesuz, W. Ji, S.F. John, C. Grimley, C. Manière, C.E.J. Dancer, Promoting microstructural homogeneity during flash sintering of ceramics through thermal management, MRS Bull. 46 (2021) 59–66. doi:10.1557/s43577-020-00010-2.

[37] M. Hasanuzzaman, A. Rafferty, A.G. Olabi, T. Prescott, Sintering and characterisation of nano-sized yttria-stabilised zirconia, Int. J. Nanoparticles. 1 (2008) 50. doi:10.1504/IJNP.2008.017618.

[38] R. Raj, M. Cologna, A.L.G. Prette, V. Sglavo, Methods of flash sintering, Patent US 20130085055 A1, US 20130085055 A1, 2013.

https://www.google.com/patents/US20130085055.

[39] C. Maniere, L. Durand, C. Estournès, Use of a deformable interface for the production of complex parts, Patent WO2017077028 A1, Patent WO2017077028 A1, 2015.

[40] C. Manière, L. Durand, A. Weibel, C. Estournès, Spark-plasma-sintering and finite element method: From the identification of the sintering parameters of a submicronic α -alumina powder to the development of complex shapes, Acta Mater. 102 (2016) 169–175. doi:10.1016/j.actamat.2015.09.003.

[41] K. Matsugi, H. Kuramoto, O. Yanagisawa, M. Kiritani, A case study for production of perfectly sintered complex compacts in rapid consolidation by spark sintering, Mater. Sci. Eng. A. 354 (2003) 234–242. doi:10.1016/S0921-5093(03)00012-1.

[42] T. Voisin, J.-P. Monchoux, L. Durand, N. Karnatak, M. Thomas, A. Couret, An Innovative Way to Produce γ-TiAl Blades: Spark Plasma Sintering, Adv. Eng. Mater. 17 (2015) 1408–1413. doi:10.1002/adem.201500019.

[43] C. Manière, L. Durand, A. Weibel, G. Chevallier, C. Estournès, A sacrificial material approach for spark plasma sintering of complex shapes, Scr. Mater. 124 (2016) 126–128. doi:10.1016/j.scriptamat.2016.07.006.

[44] E.A. Olevsky, C. Garcia-Cardona, W.L. Bradbury, C.D. Haines, D.G. Martin, D. Kapoor, Fundamental Aspects of Spark Plasma Sintering: II. Finite Element Analysis of Scalability, J. Am. Ceram. Soc. 95 (2012) 2414–2422. doi:10.1111/j.1551-2916.2012.05096.x.

[45] C. Maniere, A. Pavia, L. Durand, G. Chevallier, V. Bley, K. Afanga, A. Peigney, C. Estournès, Pulse analysis and electric contact measurements in spark plasma sintering, Electr. Power Syst. Res. 127 (2015) 307–313. doi:10.1016/j.epsr.2015.06.009.

[46] X. Wei, D. Giuntini, A.L. Maximenko, C.D. Haines, E.A. Olevsky, Experimental Investigation of Electric Contact Resistance in Spark Plasma Sintering Tooling Setup, J. Am. Ceram. Soc. 98 (2015) 3553–3560. doi:10.1111/jace.13621.

[47] C. Manière, L. Durand, E. Brisson, H. Desplats, P. Carré, P. Rogeon, C. Estournès, Contact resistances in spark plasma sintering: From in-situ and ex-situ determinations to an extended model for the scale up of the process, J. Eur. Ceram. Soc. 37 (2017) 1593–1605. doi:10.1016/j.jeurceramsoc.2016.12.010.

Acknowledgements

The support of the US National Science Foundation, Division of Materials Research (Award No. 1900876) is gratefully acknowledged.

Data availability

The authors declare that the data supporting the findings of this study are available from the corresponding author upon a reasonable request.

Author contributions

CM and EO managed the overall project. C.M. and G.L. conducted the SPS experiments. G.L conducted all the SEM characterizations. C.M. performed the finite element simulations. C.M. wrote the paper with input from G.L. and E.O. E.O. refined the paper. All authors contributed to the interpretation of the results.

Conflict of Interest

Competing interests: The authors declare no competing financial interests.

Biographies

Charles MANIERE completed his PhD at the University of Toulouse specialising in the modeling of Spark Plasma Sintering. From 2016 to 2018 he completed a 2 year PostDoc at San Diego State University. During this PostDoc, Charles developed advanced multiphysics models for microwaves sintering, flash sintering, and additive manufacturing. He is the author of 50 scientific publications. In 2018, he succeeded in the selective entry of the CNRS and started his current position as an assistant scientist at the CRISMAT laboratory (Normandie Université) where he is developing his activity in sintering.

Geuntak Lee is materials researcher and engineer specialized in material processing, manufacturing, and characterization. During his Ph.D. studies, he identified the effect of the electric current on powder processing and optimized the electric current pathway to achieve rapid densification of metal and ceramic powders. He is the author of 21 peer-reviewed papers and 1 US patent.

Eugene Olevsky is Dean and Distinguished Professor of the College of Engineering at San Diego State University. He has obtained M.S. degrees in Mechanical Engineering and Applied Mathematics and Ph.D. in Materials Engineering. He is the author of over 500 scientific publications and of more than 150 invited presentations. He has supervised more than 100 post-doctoral, graduate, and undergraduate students. Prof. Olevsky is a Fellow of the American Ceramic Society, a Fellow of the American Society of Mechanical Engineers, a Fellow of ASM International, and Humboldt Fellow; he is a Full Member of the International Institute of Science of Sintering.

Figure captions

Fig. 1 Concept of complex shape flash sintering. The ultra-rapid complex shape sintering method integrates two coupled approaches: a) the flash spark plasma sintering conditions and configuration[8] b) the complex shape deformed interface approach[18].

Fig. 2 Complex shape parts obtained by the deformed interface approach and in combination with the flash spark plasma sintering approach.

Fig. 3 Flash sintering of 30 mm zirconia gear. a) Current and displacement curves recorded during the flash spark plasma sintering experiment b) the upper part shows the sintered pellet where the gear shape appears along with the sacrificial parts and graphite foils interface, the lower part shows the released gear shape after ejection of the sacrificial parts.

Fig. 4 Physical field uniformity and correlation with obtained microstructures. The upper part (a) shows the temperature distribution and electric current lines during the electric current peak, the lower part (b) represents the SEM fracture images in the center and at the edge of the sintered sample which demonstrate a homogeneous microstructure with grain size clearly lower than 500 nm.